Online at www.e-iph.co.uk
Indexed in Clarivate Analytics WoS,

E-B
Environment - Behaviour Proceedings Journal

CSSR 2023
https://cssr.uitm.edu.my/2023/

e-IPH
e-International Publishing House Ltd., United Kingdom

10th International Conference on Science & Social Research
Virtual Conference
6 - 7 Nov 2023
Organised by: Research Nexus UiTM (ReNeU), Universiti Teknologi MARA

Comparison of Structuring Elements for Benign and Malignant Classification in Breast Cancer

Siti Salmah Yasiran*, **Norazlin Mohd Noor**, **Nurul Fateha Zainal**
**Corresponding Author*

Faculty of Computer and Mathematical Sciences,
Universiti Teknologi MARA, 40450 Shah Alam, Selangor, Malaysia.

salmahyasiran@uitm.edu.my, azlinalin09@gmail.com, tehazainal77@gmail.com
Tel: +601110726300

Abstract

Computer-Aided Diagnosis (CADx) systems assist radiologists in reducing errors in breast cancer detection. Structuring elements (SEs) in mathematical morphology enhance image quality and feature extraction for tumour classification, but selecting optimal type and size is challenging. This study compares square and diamond-shaped SEs for classifying benign and malignant tumours. Mean Squared Error (MSE) is used to evaluate image quality. The highest classification accuracies were achieved at specific radii: square (width 80), 89.0%, and diamond (radius 50), 89.2%. Square SEs consistently produced lower reconstruction errors, demonstrating their robustness in morphology-based CAD systems.

Keywords: Mammogram; segmentation; breast cancer; structuring element

DOI: https://doi.org/10.21834/e-bpj.v10iSI40.7710

1.0 Introduction

Breast cancer is the most common cancer among women worldwide. In 2022, 2.3 million women were estimated to have breast cancer, with 670,000 fatalities worldwide (World Health Organisation, 2025). Women account for around 99% of the recorded breast cancer cases, while men account for only 0.5-1%. The risk of developing breast cancer increases with age; however, early detection and timely treatment can reduce the mortality rate of breast cancer if they were detected and treated early (World Health Organization, 2025). According to Lee et al. (2019), breast cancer can be detected through the identification of various clinical symptoms, including lumps or thickening in the breast or underarm area, changes in breast size or shape, nipple abnormalities, skin changes, and breast pain. In addition to clinical examination, medical imaging modalities, particularly mammography, play a crucial role in breast cancer detection. Mammography is considered the gold standard method for breast cancer screening and is widely used for routine screening programs worldwide.

Nevertheless, this modality has notable limitations. Radiologists are frequently required to evaluate large volumes of mammograms, which can contribute to diagnostic fatigue and reduce detection accuracy. This has led to the adoption of computer-aided diagnosis

eISSN: 2398-4287 © 2025. The Authors. Published for AMER by e-International Publishing House, Ltd., UK. This is an open access article under the CC BY-NC-ND license (http://c5eativecommons.org/licenses/by-nc-nd/4.0/). Peer–review under responsibility of AMER (Association of Malaysian Environment-Behaviour Researchers
DOI: https://doi.org/10.21834/e-bpj.v10iSI40.7710

(CAD) systems, which serve as a second pair of eyes for radiologists in breast cancer diagnosis (Gao et al., 2019). CAD with mammography helps differentiate benign from malignant tumours. Benign tumours are noncancerous and have cellular structures similar to normal tissue, with regular, smooth, and compact formations. In contrast, malignant tumours are cancerous, displaying abnormal, disorganised, and invasive cellular architecture (Spane & Fayed, 2023). CAD systems use mathematical morphology to extract structural features, such as shape, margin irregularity, and boundary roughness, which are essential for classifying tumours as benign or malignant (Embong & Anuar, 2019).

However, selecting an appropriate structuring element and its optimal radius for morphological processing remains challenging. Tumour structures vary significantly in size, shape, and scale, and an unsuitable choice may result in the loss of diagnostically important features or inaccurate image interpretation. In particular, the influence of different structuring element shapes and radii on tumour feature extraction remains insufficiently investigated. Therefore, this study aims to evaluate the effects of various structuring element selections and radii on morphological feature extraction and the classification of breast tumours in a computer-aided diagnosis (CAD) framework.

2.0 Literature Review

2.1 *Mathematical Morphology*

Mathematical morphology has been widely applied in breast cancer image analysis to enhance features, reduce noise, and support automated classification. Dhar (2021) employed morphological operations, including dilation and opening, on grayscale mammography images, followed by binarisation, and reported improved performance with the application of gamma correction. Similarly, Abudawood et al. (2018) combined morphology-based erosion and dilation with Local Binary Patterns (LBP) to separate breast regions from undesired objects, enhancing preprocessing and feature extraction for anomaly classification. Zhang et al. (2019) proposed Mathematical Morphological Filtering (MMF), which employs multiple structuring elements at different scales to extract scale-specific information while effectively suppressing noise, thereby outperforming conventional band-pass filters and empirical mode decomposition (EMD). Aouad and Talbot (2022) developed a binary morphological neural network (BiMoNN) that demonstrated the equivalence between classical morphological operators and convolutional neural networks. Their approach effectively integrates erosions, dilations, and anti-dilations into a trainable framework, showing promising results for medical image analysis. Collectively, these studies illustrate the versatility of morphological operations in noise reduction, feature extraction, and automated classification, forming a foundation for structuring element design in CAD systems.

2.2 Structuring Elements

Structuring elements (SEs) are fundamental components in mathematical morphology and play a critical role in determining how morphological operations interact with image structures. Morphological operations are a non-linear image preprocessing method, in which the size and shape of the structuring element are defined relative to the features of interest rather than the overall image size. Common SE shapes include flat geometries such as linear, square, disc, rectangle, and diamond shapes, as well as non-flat forms such as ball-shaped elements (Kumar et al., 2020). This study represents structuring elements as binary matrices consisting of zeros and ones, where the configuration defines the spatial relationship between the structuring element and the image pixels. Morphological operations such as dilation, erosion, opening, and closing utilise structuring elements to probe and transform image features through many iterations. Opening and closing are composite operations that combine erosion and dilation to remove imperfections, smooth object contours and extract and preserve meaningful structural information. The effectiveness of these operations depends heavily on the chosen structuring element.

Previous studies have shown that the selection of structuring element shape and size critically influences the outcome of morphological feature extraction. For example, Ghosh et al. (2024) developed trainable multi-scale structuring elements that adapt to variations in region-of-interest shape and size, demonstrating the limitations of fixed, predefined structuring elements. Similarly, recent morphology-based detection methods for breast microcalcifications have emphasised the importance of selecting appropriate structuring element sizes to handle lesion size diversity effectively (Touil et al., 2020). However, despite these findings, the selection of the structuring element (SE) shape and size is often treated as a fixed or heuristic choice. Although numerous studies utilise predefined or adaptive structuring elements, the impact of classical structuring element shapes and their associated radii on classification performance has not been systematically investigated. Limited attention has been given to comparing commonly used flat geometries, such as square and diamond-shaped structuring elements, across multiple scales in benign–malignant tumour classification tasks. Furthermore, the interaction between SE geometry, dimensionality reduction techniques such as PCA, and computational efficiency remains underexplored. The present study addresses this gap by providing a focused comparative analysis of square and diamond-shaped structuring elements across varying sizes, evaluating their impact on classification accuracy, reconstruction error, and computational efficiency within a CADx framework.

3.0 Methodology

Fig. 1 shows the CADx method for breast tumor classification.

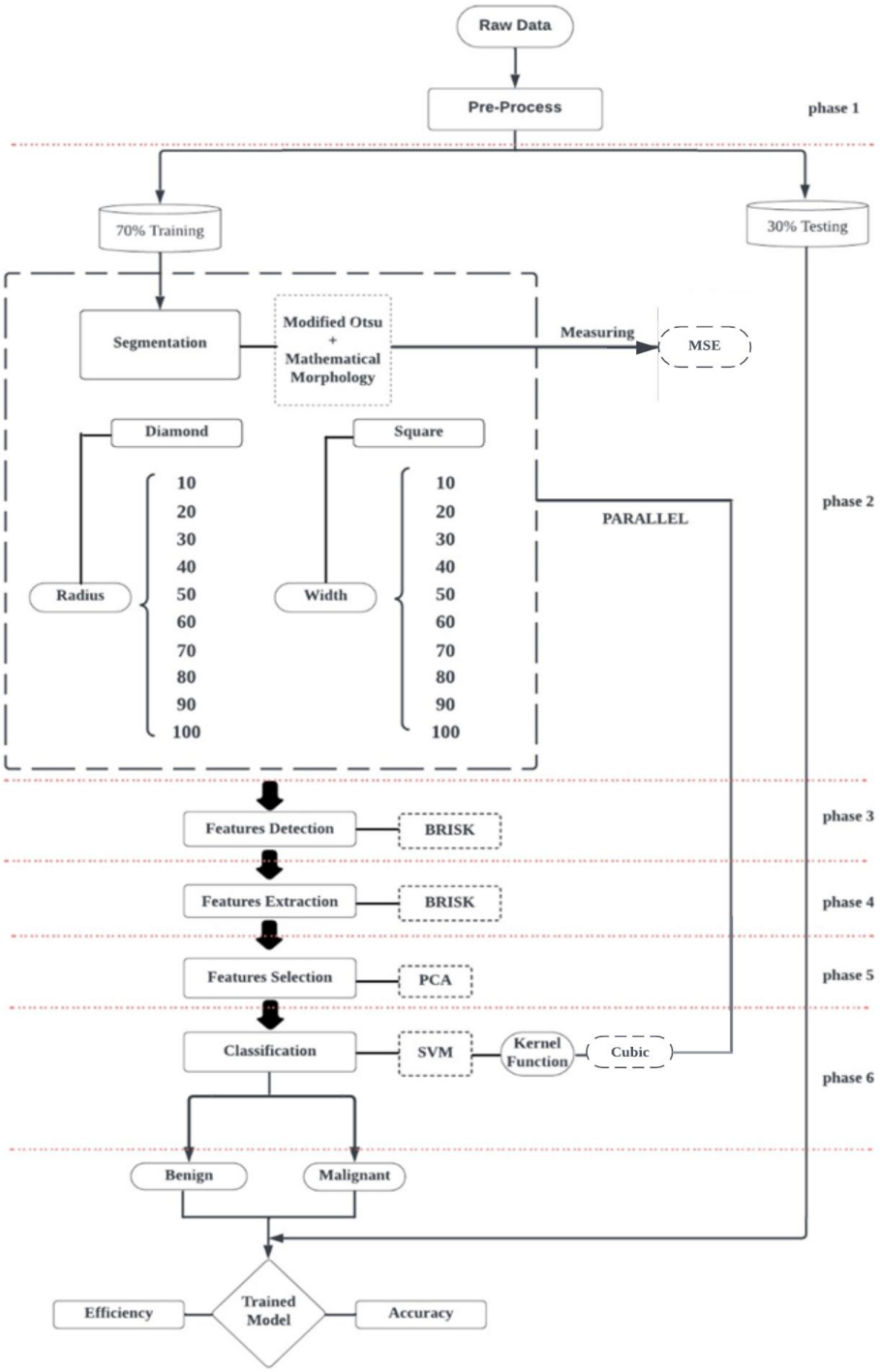

Fig. 1: The proposed method of the CADx system

As shown in Fig. 1, CADx involves six significant phases. As mentioned earlier, this study focuses on the segmentation phase, which is in phase 2. In the first phase, the data is downloaded from the open-source database by the Mammographic Image Analysis Society (MIAS). The dataset includes 109 mammography images, each with corresponding annotations specifying breast tumour locations. There are 50 malignant and 59 benign. The dataset is split into 70% for training and 30% for testing, following the approach suggested by Forman and Cohen (2004). As indicated by the dashed box in the figure, this study focuses on the segmentation component. The segmentation stage employed the Modified Otsu method and mathematical morphology using 70% of the dataset for training. In the

mathematical morphology process, diamond-shaped and square-shaped structuring elements are utilised. Ten different radii of the diamond-shaped structuring element and ten widths of the square-shaped structuring element are implemented, and the resulting image quality is evaluated using the mean squared error (MSE). Feature detection and extraction are performed in Phases 3 and 4, respectively. Both are using BRISK features. After that, PCA is applied in the feature selection phase. Phase 6 represents the final stage, in which benign and malignant tumour classification is performed using an SVM classifier with a cubic kernel. From phase 2 to phase 6, this study utilised parallel mode on the working models. After all six phases are completed, the best-trained model, as determined by accuracy and efficiency metrics, is evaluated using a 30% testing dataset. Assessing the two performance metrics across both datasets enables a systematic comparison of diamond- and square-shaped structuring elements.

3.1 Phase 1: Preprocessing

Preprocessing can enhance digital mammography images by removing impulsive noise at tissue boundaries. Improving mammogram image quality enhances image contrast by reducing noise, thereby facilitating the detection of anomalies. According to Kumar et al. (2020), image preprocessing improved brightness and amplified the distinction between the ground truth regions and surrounding tissue. This study utilises an open database, the MIAS Mini Mammographic Database, which can be downloaded as an open source.

3.2 Phase 2: Segmentation

Preprocessing can enhance digital mammography images by removing impulsive noise at tissue boundaries. Improving mammogram image quality can increase contrast by reducing noise, enabling the detection of anomalies. According to Kumar et al. (2020), preprocessing enhanced image brightness and improved the contrast between the ground. This study utilises an open database, the MIAS Mini Mammographic Database, which can be downloaded as an open source.

3.2.1 Modified Otsu

After the binarisation, this study applied the Modified Otsu method. According to Yasiran et al. (2020), the Modified Otsu technique is based on an iterative process in which all potential threshold values are evaluated, and the dispersion of pixel intensity levels on either side of the threshold is quantified. Unlike the original Otsu method, which relies on within-class variance, the Modified Otsu approach employs standard deviation as the criterion for threshold selection. They have found that the modified Otsu method produces promising results.

3.2.2 Mathematical Morphology

Morphological erosion is utilised to suppress extrusions by shrinking the segmented region, thereby refining the segmentation result. Through the structuring of components, the function *f* provides the erosion of the image f. The origin of the structuring element is at *(x, y)*, and the new pixel value is determined by using the rule that *x* and *y* are the intensities in the image. In this study, erosion is performed using a 3 × 3 square structuring element.

The erosion of *A* by *B* is defined in the basic mathematical definition.

$$\left[A\Theta B\right]=\left\{x\,|\,(B)_x\cap A^c\neq\varnothing\right\} \tag{1}$$

Where A is a set of input image coordinates, B is a set of structuring element coordinates, and $(B)_x$ is a translation of *B* so that its origin is at *x*. According to Kisačanin and Schonfeld (1994) and Aouad and Talbot (2022), they have developed a threshold linear convolution representation to depict morphological operations quickly. They limit the binary and dimensional discrete functions $\left\{g(x)\in\{0,1\}:x\in Z^n\right\}$. The erosion $\left[g\Theta s\right](x)$ of a function $g(x)$ by a structuring element $s(x)$ is given by

$$\left[g\Theta s\right](x)=\boxtimes_{\{y\in Z^n:s(y)=1\}}g(x-y) \tag{2}$$

The threshold linear convolution represents erosion. The threshold $h_\beta(\boxtimes)\ \beta\in\boxtimes$ is:

$$h_\beta(x)=\begin{cases}0, & x\leq\beta\\ 1, & x>\beta\end{cases} \tag{3}$$

for every $x\in\boxtimes$. The linear convolution $\left[g_1*g_2\right](x)$ of function g_1 and g_2 is given by

$$\left[g_1 * g_2\right](x) = \Sigma_{y \in Z^n}\left[g_1(x-y) \cdot g2(y)\right] \quad (4)$$

for every $x \in Z^n$. Then, they provide a threshold linear convolution representation of the erosion.

$$\left[g \Theta s\right](x) = \left(h_\beta\left[g^c * s\right](x)\right)^c \quad (5)$$

Equation (9) proves that the thresholder linear convolution can represent erosion. According to Dhar (2021), two input data sets are needed by the erosion operator. The first image represents the input image to be eroded. Another type of structuring element is defined as a collection of coordinate points and is generally small in size. It is also referred to as a kernel. This structural component creates the erosion's effect on the image.

3.2.2.1 Structuring Element of Square

A square-shaped structuring element of width W pixels is created using the MATLAB function SE = strel('square', W), where W W denotes the width of the square structuring element and must be specified as a positive integer.This stage represents the point in the process at which the adjustments are introduced. Fig. 2 shows the square SE with a width of 3 in binary form.

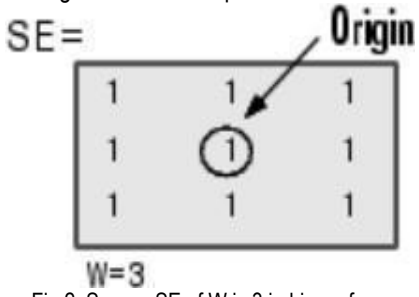

Fig.2: Square SE of W is 3 in binary form
(Source: Image from http://www. ece. Northwestern. edu/local-apps/matlabhelp/toolbox/images/strel. html#223506)

As illustrated in Fig. 2, the origin of the structuring element is typically considered to be at the center of the matrix, even if it lies outside the element. According to Primkhajeepong et al. (2010), morphological operations have been used to categorise the different cancer cells that might be found in breast cancer. Opening processes are one of them that can remove the identified healthy cell. It was observed that segmentation using a city block distance transform with a four-pixel width produced optimal results when square-shaped structuring elements were applied, achieving 85% segmentation performance and 94% accuracy in breast cancer cell counting classification.

3.2.2.2 Structuring Element of Diamond

A diamond-shaped structuring element with a radius of R.This study uses diamond-shaped syntax from MATLAB, SE= strel('diamond', R), where R specifies the distance from the structuring element origin to the points of the diamond. Here are the adjustments that have been made. Fig. 3 shows the diamond SE with radius 3 in binary form.

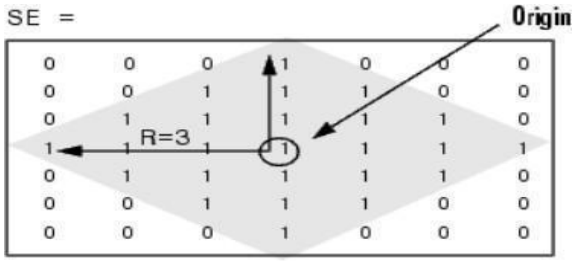

Fig. 3: Diamond SE of R is 3 in binary form
(Source: Image from http://www. ece. Northwestern. edu/local- apps/matlabhelp/toolbox/images/strel. html#223506)

Fig. 3 shows that the centre of the diamond, which consists of '1', is the origin of the shape. The radius is counted by excluding the origin. Since breast cancer anomalies are typically uncommon, diamond structure elements can accommodate them. The application of structuring elements, along with diamond and morphological filtering, contributes to the enhancement of image features.

3.0 Results and Discussion

The performance of the CADx system was assessed using diamond- and square-shaped structuring elements for benign and malignant tumour classification.The dataset was divided into 70% for training and 30% for testing. Classification accuracy and computational efficiency were analysed with and without PCA to assess the influence of dimensionality reduction on feature representation.

4.1 Effect of structuring Element Size and Shape on Classification Accuracy

The results of feature extraction and detection using BRISK on the training dataset, both with and without principal component analysis (PCA), are presented in Tables 1 and 2.

Table 1: Result of the square structuring element

Width	with PCA			without PCA		
	Accuracy (%)	Efficiency		Accuracy (%)	Efficiency	
		OBS/SEC	SECS		OBS/SEC	SECS
10	86.9	~1500	436.36	88.1	~1100	704.85
20	88.4	~2000	517.86	87.2	~1400	849.65
30	87.4	~840	1120.5	86.2	~330	1231
40	87.3	~350	1266.7	85.6	~400	1126.7
50	87.9	~1100	1099.7	87.3	~320	1229.2
60	86.8	~650	1863.5	88.3	~370	1982.7
70	87.3	~580	1069.8	84.8	~270	1052.6
80	88.9	~1500	1078.6	89.0	~1700	1187.47
90	87.0	~1500	755.27	86.0	~1100	777.47
100	87.2	~1500	811.87	86.9	~550	764.66

As presented in Table 1, the square-shaped structuring element attained its highest classification accuracy at a width of 80, achieving 88.9% with PCA and 89.0% without the application of PCA. This suggests that intermediate SE size is optimal for capturing relevant tumour features, while excessively small or large widths may either miss structural details of oversmooth lesion boundaries.

Similarly, Table 2 shows that the diamond-shaped structuring element achieved its best performance at a radius of 50, with accuracies of 88.9% (with PCA) and 89.2% (without PCA). The comparable peak accuracies across both structuring element shapes imply that the size of the structuring elements is the dominant factor influencing performance, whereas the shape exerts a comparatively subtle effect on feature preservation.

Table 2: Result of the diamond structuring element

Radius	with PCA			without PCA		
	Accuracy (%)	Efficiency		Accuracy (%)	Efficiency	
		OBS/SEC	SECS		OBS/SEC	SECS
10	88.4	~1900	466.4	86.8	~1300	764.66
20	88.0	~1200	634.75	87.8	~1200	1000.6
30	87.3	~1700	378.2	87.9	~800	824.53
40	88.7	~1200	155.3	88.1	~860	175.11
50	88.9	~1800	526.7	89.2	~1400	554.75
60	88.7	~2200	991.49	86.9	~1400	708.22
70	87.6	~920	578.7	87.4	~1000	943.48
80	88.0	~1100	133.37	88.2	~700	946.02
90	85.7	~1700	376.64	84.8	~1100	336.18
100	87.6	~1500	337.29	87.7	~1300	422.65

The results also show that PCA does not consistently improve classification accuracy, suggesting that morphological features extracted using appropriate SE sizes already contain discriminative information for benign–malignant differentiation.

4.2 Effect of Structuring Element Size and Shape on Classification Accuracy

For the benign testing dataset (17 images) (Table 3), several images (the grey -highlighted: mdb204, mdb218, mdb222, mdb227, mdb252, mdb290, mdb314) exhibited zero MSE for both square and diamond SEs, indicating robust morphological representation regardless of shape. However, among images with non-zero error, square-shaped structuring elements generally resulted in lower mean squared error (MSE) values compared to other shapes.

Table 3: MSE values in the benign class for the testing dataset

Id image	MSE	
	Square SE	Diamond SE
mdb204	0	0
mdb207	1.52323	**0.833404**
mdb214	41.1450	**39.77713**
mdb218	0	0
mdb219	**10.18217**	12.50447
mdb222	0	0
mdb223_1	**85.36682**	124.59231
mdb223_2	**3.77163**	4.26382
mdb227	0	0
mdb236	**5.44549**	12.62294
mdb240	**2.06585**	2.47966
mdb244	**0.96358**	1.08899
mdb252	0	0
mdb290	0	0
mdb312	56.28166	**39.43247**
mdb314	0	0
mdb315	**0.92787**	2.77074

Benign tumours are typically characterised by smooth, well-defined, and compact structures, which align well with the isotropic nature of square-shaped structuring elements. This suggests that square SEs may preserve homogeneous texture patterns and regular boundaries commonly found in benign lesions. Diamond SEs performed better in a limited number of benign cases (mdb207, mdb214, mdb312) produce better qualities, indicating that their diagonal connectivity may occasionally capture acceptance structural variations not fully preserved by square elements.

4.2 Analysis of Reconstruction Error in Malignant Tumours

For malignant tumours (15 images) (Table 4), most images again demonstrated zero reconstruction error for both SE shapes (grey-highlighted rows). Among the remaining cases, square SEs achieved lower MSE values in the majority of images, while diamond SEs performed better only in a small subset (mdb241, mdb264).

Table 4: MSE values in the malignant class for the testing dataset

Id image	MSE	
	Square SE	Diamond SE
mdb223_2	**3.77163**	4.26382
mdb231	0	0
mdb238	0	0
mdb239_1	**0.12994**	1.05010
mdb241	3.25793	**2.14933**
mdb249_1	0	0
mdb249_2	0	0
mdb253	**0.82025**	1.81129
mdb256	0	0
mdb264	5.86572	**3.77645**
mdb267	0	0
mdb270	**1.21933**	5.33759
mdb271	0	0
mdb274	0	0
mdb293_2	**2.62095**	4.52734

Malignant tumours typically exhibit irregular shapes, spiculated margins, and heterogeneous textures. While diamond SEs may be expected to better follow diagonal or irregular structures, the results indicate that square SEs provide more stable morphological representation across a wider range of malignant cases. This suggests that square SEs may offer greater robustness when dealing with diverse tumour morphologies.

4.4 Implications for CAD System Design

Overall, the findings demonstrate that structuring element selection has a measurable impact on both classification accuracy and image reconstruction quality. While both square and diamond SEs can achieve comparable peak accuracies when appropriately sized, square SEs consistently yield lower reconstruction errors for both benign and malignant tumours. This suggests that square structuring elements offer greater stability in morphological processing.

Thus, in clinical settings where interpretability and computational efficiency are critical, morphology-based CAD systems using appropriately sized square structuring elements may offer a practical solution for supporting radiologists in tumour characterisation, particularly in resource-limited environments. Moreover, the observed dependence of optimal performance on structuring element size and shape highlights the importance of careful parameter selection during system deployment, as arbitrary or default structuring element choices may lead to suboptimal performance and reduced diagnostic reliability.

3.0 Conclusion

This study examined the effect of square- and diamond-shaped structuring elements in a morphology-based CAD framework using Modified Otsu thresholding and mathematical morphology. The proposed model achieved the highest classification accuracy without PCA, attaining 89.0% with the square structuring element and 89.2% with the diamond structuring element. While both shapes attained comparable peak accuracy, square structuring elements demonstrated more consistent performance across both benign and malignant cases. In contrast, diamond-shaped elements achieved optimal results only at specific radii. Although this study is limited to two flat structuring element geometries evaluated over fixed size ranges, and the dataset size and evaluation metrics were restricted to accuracy, efficiency, and MSE, the findings provide practical insight into the impact of structuring element selection on CAD performance. Future work may broaden the scope of this study by examining additional two-dimensional structuring elements, such as disks, rectangles, octagons, and line-based configurations, and by integrating clinically relevant performance metrics, including sensitivity and the area under the receiver operating characteristic curve (AUC).

Acknowledgement

The author(s) would like to acknowledge the Research Nexus UiTM (ReNeU) and Faculty of Computer and Mathematical Sciences, Universiti Teknologi MARA, 40450 Shah Alam, Selangor, Malaysia, for their support and contributions.

Paper Contribution to Related Field of Study

This study contributes to breast cancer CAD research by systematically comparing classical structuring element shapes and sizes, an aspect often overlooked in prior work. An evaluation of square- and diamond-shaped structuring elements was conducted across multiple radii to investigate their influence on classification accuracy, image reconstruction performance, and image quality. The results show that square SEs provide more consistent performance across benign and malignant tumours. These findings offer practical guidance for selecting structuring elements and reinforce the value of mathematical morphology in CAD system design

References

Abudawood, T., Al-Qunaieer, F. S., & Alrshoud, S. R. (2018). An Efficient Abnormality Classification for Mammogram Images. 21st Saudi Computer Society National Computer Conference (NCC), Riyadh, Saudi Arabia, 1–6. https://doi.org/10.1109/ncg.2018.8593208

Aouad, T., & Talbot, H. (2022). Binary Morphological Neural Network. In 2022 IEEE International Conference on Image Processing (ICIP). https://doi.org/10.1109/icip46576.2022.9897474

Blyss Splane, & Lisa Fayed. (2023, May 23). Malignant vs. Benign Tumours: What Are the Differences? Verywellhealth.

Dhar, P. (2021). A method to detect breast cancer based on morphological operation. International Journal of Education and Management Engineering, 11(2), 25.

Embong, R., & Anuar, S. R. (2019). Structuring Elements in the Watershed Algorithm for the Segmentation of Mammography Images. IEEE Region 10 Annual International Conference, Proceedings/TENCON, 2018-October. https://doi.org/10.1109/TENCON.2018.8650121

Forman, G., & Cohen, I. S. (2004). Learning from Little: Comparison of Classifiers Given Little Training. In Lecture Notes in Computer Science (pp. 161–172). https://doi.org/10.1007/978-3-540-30116-5_17

Gao, Y., Geras, K. J., Lewin, A. A., & Moy, L. (2019). New Frontiers: An Update on Computer-Aided Diagnosis for Breast Imaging in the Age of Artificial Intelligence. AJR. American journal of roentgenology, 212(2), 300–307. https://doi.org/10.2214/AJR.18.20392

Gholamy, A., Kreinovich, V., & Kosheleva, O. (2018). Why 70/30 or 80/20 Relation Between Training and Testing Sets : A Pedagogical Explanation. Departmental Technical Reports (CS), 1–6.

Ghosh, S., & Das, S. (2024). Multi-scale morphology-aided deep medical image segmentation. Engineering Applications of Artificial Intelligence, 137, 109047.

Kisačanin, B., & Schonfeld, D. (1994). A fast thresholded linear convolution representation of morphological operations. IEEE Transactions on Image Processing, 3(4), 455–457. https://doi.org/10.1109/83.298399

Kumar, S., Adarsh, A., Kumar, B., & Singh, A. K. (2020). An automated early diabetic retinopathy detection through improved blood vessel and optic disc segmentation. Optics and Laser Technology, 121. https://doi.org/10.1016/j.optlastec.2019.105815

Lee, M. S., Azmiyaty Amar Ma'Ruf, C., Izhar, D. P. N., Ishak, S. N., Jamaluddin, W. S. W., Ya'Acob, S. N. M., & Kamaluddin, M. N. (2019). Awareness on breast cancer screening in Malaysia: A cross sectional study. BioMedicine (France), 9(3). https://doi.org/10.1051/bmdcn/2019090318

Liu, Y., Zhang, H., Guo, H., & Xiong, N. N. (2018). A FAST-BRISK feature detector with depth information. Sensors (Switzerland), 18(11). https://doi.org/10.3390/s18113908

Nida, N., Irtaza, A., Javed, A., Yousaf, M. H., & Mahmood, M. T. (2019). Melanoma lesion detection and segmentation using deep region based convolutional neural network and fuzzy C-means clustering. International Journal of Medical Informatics, 124(January), 37–48. https://doi.org/10.1016/j.ijmedinf.2019.01.005

Primkhajeepong, C., Phukpattaranont, P., Limsiroratana, S., Boonyaphiphat, P., & Kayasut, K. (2010). Performance evaluation of automated algorithm for breast cancer cell counting. International Journal of Computer and Electrical Engineering. https://doi.org/10.7763/ijcee.2010.v2.204

Touil, A., Kalti, K., Conze, P. H., Solaiman, B., & Mahjoub, M. A. (2020). Automatic detection of microcalcification based on morphological operations and structural similarity indices. Biocybernetics and Biomedical Engineering, 40(3), 1155-1173.

World Health Organization. (2025, August 14). Breast cancer. WHO. https://www.who.int/news-room/fact-sheets/detail/breast-cancer

Yasiran, S. S, Salleh, & S., & M. R. (2020). Standard Deviation Based Otsu for Breast Cancer Classification. ASM Sci. J. ASM Sci. J.

Zhang, J., Zeng, Z., Zhang, L., Lu, Q., & Wang, K. (2019). Application of mathematical morphological filtering to improve the resolution of Chang'E-3 lunar penetrating radar data. Remote Sensing, 11(5), 524.